

NASA Technical Memorandum 85716

NASA-TM-85716 19840010984

REMOVE FROM THIS ROOM

# Noise-Reduction Measurements on Stiffened and Unstiffened Cylindrical Models of an Airplane Fuselage

Conrad M. Willis and William H. Mayes

FEBRUARY 1984

**NASA**



NASA Technical Memorandum 85716

Noise-Reduction Measurements  
on Stiffened and Unstiffened  
Cylindrical Models of an  
Airplane Fuselage

Conrad M. Willis and William H. Mayes

*Langley Research Center  
Hampton, Virginia*



National Aeronautics  
and Space Administration

**Scientific and Technical  
Information Office**

1984



## SUMMARY

As part of an airplane interior-noise study, noise-reduction measurements have been made on stiffened and unstiffened model fuselages that were cylindrical in shape. The models were tested in a reverberant-field noise environment in an unlined bare-metal configuration and a configuration which had acoustic insulating material added along with a partition to represent the fuselage floor. The cylindrical models were 50.8 cm in diameter and 124.5 cm in length and were exposed to pink noise over a frequency range from 20 Hz to 6 kHz. An unstiffened metal fuselage having a 1.6-mm-thick sidewall provided more noise reduction than a fuselage having the same sidewall weight divided between skin and stiffening stringers and ring frames. The addition of acoustic insulation to the models tended to smooth out the interior-noise spectrum by reducing or masking the noise associated with the structural response at some of the resonant frequencies.

## INTRODUCTION

The prediction and reduction of airplane interior noise have received increasing attention in recent years. Progress has been made in developing analytical prediction techniques and improved acoustic materials for reducing the noise, especially for turbofan-powered airplanes. Refinements to these prediction techniques are continuing topics of research in order to reduce the weight of acoustic material required for noise control and to provide a better understanding of the basic mechanisms involved in the transmission of noise to the airplane interior. It has also been recognized that the interior noise of propeller-driven airplanes is generally higher and more difficult to control than that of turbofan-driven airplanes (ref. 1) because the spectrum is dominated by low-frequency tones associated with the propeller blade-passage noise. Renewed interest in propeller airplanes for commercial-passenger use as a fuel-conservation measure has contributed to the increased need for a better understanding of the noise-transmission process and noise-control techniques.

The state of the art for general aviation noise-source characterization, passenger-comfort criteria, and commonly used types of noise-reduction techniques is reviewed by Wilby in reference 1. Additional factors involved in controlling the interior noise of multiengine propeller airplanes are discussed by Metzger in reference 2. These factors include the effects of propeller synchronization and the direction of propeller rotation.

An analytical study of airplane interior-noise prediction is currently being carried out by Pope in parallel with the present experimental study. The basic theory and validation experiments for an unstiffened cylindrical-fuselage model were reported in references 3 and 4. The theory was expanded in reference 5 to account for stiffened-fuselage structures and propeller-generated noise fields.

The purpose of the present report is to present experimental results of noise reduction measured in the laboratory on stiffened and unstiffened models of an airplane fuselage. The models were cylindrical in shape and were tested with and without floors and interior linings of acoustic material. The noise-reduction measurements were made in a reverberant noise field by using a speaker to apply a pink-noise

loading to the fuselage exterior. The measured noise reduction is compared with predictions by Pope from reference 5 and with the calculated values of noise reduction due to the mass of the fuselage sidewall. Also presented are the measured structural and acoustic decay times used to determine the structural and acoustic loss factors for the various configurations of the fuselage.

#### SYMBOLS AND ABBREVIATIONS

CRT	cathode-ray tube
DVM	digital voltmeter
h	distance from microphone to end of interior cavity of fuselage (see fig. 1(b)), m
L	length of fuselage interior, 119.4 cm
m	mass per unit area, $\text{kg/m}^2$
NR	noise reduction, dB
OASPL	overall sound pressure level, dB
R	radius of fuselage interior, m
r	radial location, m
SPL	sound pressure level, dB
$T_R$	reverberation time, time required for acoustic or structural vibration to decay 60 dB, sec
$\rho c$	characteristic impedance of air, rayls (where $c$ is acoustic velocity in air and $\rho$ is density of air)
$\tau$	field-incidence transmission-loss coefficient, $[0.956(m\omega/2\rho c)^2]^{-1}$ $\times \ln \left[ \frac{1 + (m\omega/2\rho c)^2}{1 + 0.0432(m\omega/2\rho c)^2} \right]$
$\phi$	angular location of microphone, measured from seam in fuselage wall (see fig. 1(b)), deg
$\omega$	circular frequency, rad/sec

#### MODELS AND TEST APPARATUS

The two model fuselages tested were aluminum cylinders with closed ends. The fuselage exterior diameter was 50.8 cm and the length was 124.5 cm. Testing was

conducted in a large reverberation room having a reverberation time of about 8 sec at approximately 2 kHz. A schematic diagram showing the arrangement of the apparatus in the test facility is presented in figure 1(a). Additional details on the acoustic characteristics of the reverberation room are given in references 6 to 8. Pink noise was generated by a 100-W speaker, and the actual level incident on the model fuselage was measured by two microphones mounted at a distance of 25 cm from the fuselage wall. Figure 1(b) shows the model-mounting arrangement and nomenclature of the coordinates specifying interior-microphone locations. The fuselage was suspended at a convenient working height by elastic cords attached to a wooden support fixture. The fuselage radius passing through the seam in the wall was designated as the  $\phi = 0^\circ$  reference line used to specify the azimuthal location of the interior microphones. Longitudinal microphone location was specified by  $h$ , the distance from the microphone to the end of the interior cavity of the fuselage.

Some geometry and fabrication details of the two fuselage models are presented in figure 2. Figure 2(a) presents details of the unstiffened model with the floor removed and also gives the radial locations of the interior microphones. The model was cylindrical and had a one-piece aluminum skin that was 0.163 cm thick; the longitudinal seam was formed by butting the edges of the skin together and epoxy-bonding over the joint an exterior strap of the same thickness as the skin. Dimensions of the cylindrical interior cavity are 50.5 cm in diameter and 119.4 cm in length. Both ends of the fuselage were closed by aluminum plates 1.3 cm thick to simulate fixed boundary conditions for the shell and to reduce the amount of flanking sound transmission. The end plates were made with removable center pieces to give working access to the fuselage interior for adjustment and calibration of instrumentation. Six 0.6-cm-diameter condenser microphones were mounted on a radially oriented bar attached to a tube on the fuselage centerline. Microphone location was adjusted by rotating and translating the tube. The tube passed through close-fitting bushings on the fuselage ends to reduce flanking of sound into the fuselage. Construction details for the stiffened model are presented in figure 2(b). The stiffened and unstiffened models had approximately the same weight. Skin thickness for the stiffened model was about one-fourth of that of the unstiffened model, and the stringers and ring frames were approximately equal in weight. The stringers were inside the fuselage, but the ring frames were placed on the outside of the skin to reduce fabrication cost and time.

Fabrication details of the floor and additional information on the lining installed in the stiffened model for part of the tests are presented in figure 2(c). The floor was 0.08 cm thick, had two longitudinal stiffeners, and was supported at the ends. Additional floor support was obtained by attaching the floor to the skin with silicone rubber. The rubber also provided a seal between the interior volumes above and below the floor. The acoustic material used to line this configuration consisted of a 1.3-cm-thick layer of fiberglass having a mass of  $0.22 \text{ kg/m}^2$  and a layer of lead-vinyl material having a mass of  $2.4 \text{ kg/m}^2$ . The fiberglass was laid on the skin and was covered with a layer of lead-vinyl material. The lining material was held in place by flexible plastic retainer strips that were bent into an arc by the buckling pressure of the ends pressing against the stringers. (See fig. 2(c).) The sidewall was completely covered except for the radial legs of the stringers whose bare tops extended through the lining. The same lining material was also applied to the underside of the floor, but the order was reversed to simplify installation. The cloth side of the lead-vinyl lining was cemented to the metal, and the fiberglass

facing was cemented to the lead-vinyl lining. The model cover plate was lined with a 1.3-cm-thick layer of fiberglass, but the inner surface of the end rings was unlined. A photograph of the stiffened model is presented in figure 3.

Lining for the unstiffened model with floor consisted of a 1.3-cm-thick layer of fiberglass on the sidewall only, but the floor was unlined. Other test configurations were as follows: the unlined models without floor and the models without floor but lined with acoustic foam. A 0.6-cm-thick layer of foam was used for lining the unstiffened model, and a 1.9-cm-thick layer was used for lining the stiffened model.

#### INSTRUMENTATION AND TEST PROCEDURE

A schematic diagram indicating the instrumentation used to acquire and reduce the data is presented in figure 4. The output from a signal generator was passed through a power amplifier to a 100-W speaker to provide the exterior-noise loading on the model. Two exterior microphones were located near the model to measure the impinging ambient noise levels. An array of six interior microphones were mounted on a movable fixture that could be rotated and translated to make measurements at any desired point in the model interior. Microphone output was passed one channel at a time through a selector switch to a digital voltmeter and a one-third-octave spectrum analyzer. Data storage and processing capability was provided by connecting the analyzer memory to a plotter, digital tape recorder, and a minicomputer. A few lightweight accelerometers were glued to the structure for one part of the test to obtain data on structural damping.

One or more speakers were mounted near a corner of the reverberation room and the model was placed 4 m away. The noise spectra for the area surrounding the model were surveyed and minor adjustments were made to the locations of the model and speakers in an attempt to locate the model within a noise field having fairly uniform low-frequency intensity on all sides. Noise intensity level at frequencies above 50 Hz was uniform throughout the test room. The exterior microphones were located on opposite sides and near opposite ends of the model at a distance of 0.3 m from the model to avoid including the effects of the surface reflections in the measured intensity. After setting the interior microphones at the desired test location, the speaker volume was adjusted to provide a measurable noise level inside the particular fuselage configuration being tested. Then, the OASPL for all microphones was recorded, and representative spectra were observed on the CRT screen of the analyzer and were recorded by the digital tape recorder.

In posttest processing, the taped spectra were fed back into the analyzer memory and the SPL for each band of interior noise was subtracted from exterior spectra to obtain noise reduction. The spectra were fed into a minicomputer for averaging.

#### RESULTS AND DISCUSSION

Noise-reduction spectra and overall noise reduction have been measured for a stiffened and an unstiffened simple model of a cylindrical airplane fuselage. Both fuselage models were tested as unlined bare-metal structures and also with acoustic lining material. Figure 5 presents an exterior spectrum for a typical test and the resulting interior spectra for the stiffened and unstiffened models at one particular microphone location. The exterior spectrum shown has a fairly flat spectral distribution over the range from 31 to 3150 Hz. The interior-noise-spectral data have the highest amplitude between 125 and 3150 Hz, and thus this range is of utmost interest



for the two model configurations represented in figure 5. The two interior spectra are generally similar in shape but have some large differences in amplitude at particular frequencies, for instance, 200 Hz. The differences are assumed to result from the differences in the structural modes in a given one-third-octave-band center frequency and the differences in stiffness and mass distribution between the stiffened and unstiffened fuselages. Above 500 Hz, the spectra were similar in shape but the stiffened fuselage had a slightly higher magnitude.

#### Unlined Fuselages

Noise-reduction spectra.- Spectral data averaged over the fuselage volume for the unlined bare-metal structure are presented in figure 6. Variations in interior sound pressure level were assumed to be axisymmetrically distributed; therefore, the noise levels were surveyed over only a 90° sector of the interior volume extending axially over one-half of the fuselage length. The averaged data followed the same trends previously observed in figure 5. At frequencies above 500 Hz, the differences were small but the stiffened model had a slightly lower noise reduction (or higher interior SPL) in most one-third-octave bands. Figure 7 presents comparisons of noise-reduction spectra at two radial locations to show that the radial variation is small. Most one-third-octave-band center frequencies have less than a 5-dB radial variation in SPL for both unstiffened and stiffened models.

Overall noise reduction.- The variation in overall noise reduction with microphone location for the stiffened and unstiffened fuselages is presented in figure 8. The stiffened model provided much less noise reduction, about 8 dB, as compared with about 16 dB for the unstiffened model, which had the thicker skin. Both models were a few decibels quieter near the centerline than near the skin. Spatial variations of measured OASPL in the circumferential and longitudinal directions were not significant in either model.

#### Unstiffened Fuselage With Lining

Noise-reduction spectra.- Spectra for two types of fuselage linings are presented in figure 9. Part of the spectrum for the unlined fuselage, previously presented in figure 7(a), is repeated for comparison. Spectra for the two treatments are generally similar in shape, and both produced significant increases in noise reduction over the range from 500 to 4000 Hz, where the unlined-fuselage noise reduction was lowest. Radial variation in noise reduction appears to be greater with acoustic foam lining.

Overall noise reduction.- Figure 10 presents a comparison of noise reduction for the two lining configurations with that for the unlined fuselage. Installation of a floor in the model seemed to reduce the radial variation in noise reduction. However, circumferential variation in NR was increased, probably because of the additional noise generated by vibration modes of the floor.

#### Stiffened Fuselage With Lining

Noise-reduction spectra.- Noise-reduction spectra for two radial locations on the stiffened fuselage with floor and lining are presented in figure 11, and the unlined spectrum is repeated for comparison. There is little variation in NR with

radial location over much of the frequency range. The lining provided a significant improvement in NR for most of the one-third-octave analysis bands above 31 Hz.

Spectra for the stiffened and unstiffened fuselages are presented in figure 12 to compare similarities in the spectral shapes. In the basic unlined configuration (fig. 12(a)), the peaks in the spectra for the stiffened and unstiffened models tend to occur at different frequencies, as expected, and have deep valleys between sharp peaks. In figure 12(b), the noise-reduction spectra for the two fuselages are compared after adding a floor and a lining of acoustic insulation to the basic configurations. The increase in noise reduction for the stiffened configuration was more than that for the unstiffened fuselage because the stiffened configuration received a heavier lining treatment. The two spectra appear to be somewhat more similar in shape than that for the unlined model; the spectral peaks for the two configurations match a little better in frequency and have a more rounded shape, and the valleys between peaks are not as deep. In an attempt to quantify the similarity of the compared spectra, the root-mean-square (rms) difference in decibel level was calculated after translating one spectrum in each pair enough that its arithmetic average of one-third-octave-band decibel levels was made equal to that of the other spectrum. The rms difference between spectra for the lined-fuselage condition was less than one-half that for the basic configuration. This smoothing of the spectral peaks and filling in of valleys that occurs with installation of the floor and lining tends to mask some of the fine detail of the structural response from the spectrum. Therefore, for heavy applications of acoustic lining materials, the acoustic characteristics of the lining may have more effect on interior noise reduction than the characteristics of the basic structure.

Overall noise reduction.- Figure 13 presents the circumferential variation of overall noise reduction for the stiffened fuselage with floor and lining. Most of the data fall within  $\pm 1 \frac{1}{2}$  dB of the median value. The circumferential variation appears to be a little more irregular near the center of the cylinder ( $h/L = 0.42$ ) than near the end. Figure 14 presents a comparison of the radial variation in overall noise reduction for the two lining configurations with that obtained for the unlined fuselage. The foam-lined model has a much greater noise reduction than the unlined model. However, the addition of the heavier fiberglass and lead-vinyl lining produced only minor increases over the noise reduction obtained with the foam lining.

#### Noise-Reduction Predictions

Figure 15 presents a comparison of the calculated mass-law NR with space-averaged measurements of noise reduction for lined and unlined fuselage configurations. The data shown were computed by the formula

$$NR = TL - 10 \log(S/A)$$

from equation (1) of reference 9, where TL is the transmission loss given by

$$TL = -10 \log[\tau(\omega)]$$

$\tau(\omega)$  is the field-incidence transmission coefficient, S is the surface area of the model, and A is the absorption of the model interior. This simple mass-law calcu-

lation appears to have little or nothing in common with the measured noise reduction for the unlined fuselage. (See fig. 15(a).) The calculated mass-law NR data for the lined fuselage (fig. 15(b)) appears to have roughly the same slope as the measured NR data at frequencies above 500 Hz, but the calculated NR is 5 or 10 dB high in most bands. As expected in the stiffness-controlled region below 500 Hz, the calculation is of no use in predicting noise reduction. Figure 15 also presents data from reference 5 to demonstrate that more elaborate calculations, such as the Propeller Aircraft Interior Noise (PAIN) program developed by Pope (ref. 10), can produce useful predictions of interior noise. Agreement between measurements and predictions is good above 125 Hz for the unlined fuselage (fig. 15(a)) and is good above 50 Hz for the lined fuselage (fig. 15(b)). Continuing work on the analytical model (ref. 10) has extended its capabilities to more realistic models of fuselage structures and exterior noise fields.

The analytical prediction method used by the PAIN program requires information on the structural and acoustic loss factors for the fuselage being analyzed. Figure 16 presents reverberation-time measurements made on the models by using accelerometers on the structure and microphones in the model interior acoustic space. These measurements were input to the PAIN program and were used to estimate structural damping and acoustic absorption for the models. It can be seen that both structural and acoustic reverberation times decreased with frequency and that the structural  $T_R$  varied over a somewhat wider range than the acoustic  $T_R$ . Adding the floor reduced the acoustic  $T_R$  but had little effect on the structural  $T_R$ .

#### CONCLUSIONS

Noise-reduction measurements have been made on simple models of stiffened and unstiffened cylindrical airplane fuselages. Lined and unlined configurations were tested in a reverberant-field noise environment. The results have led to the following conclusions:

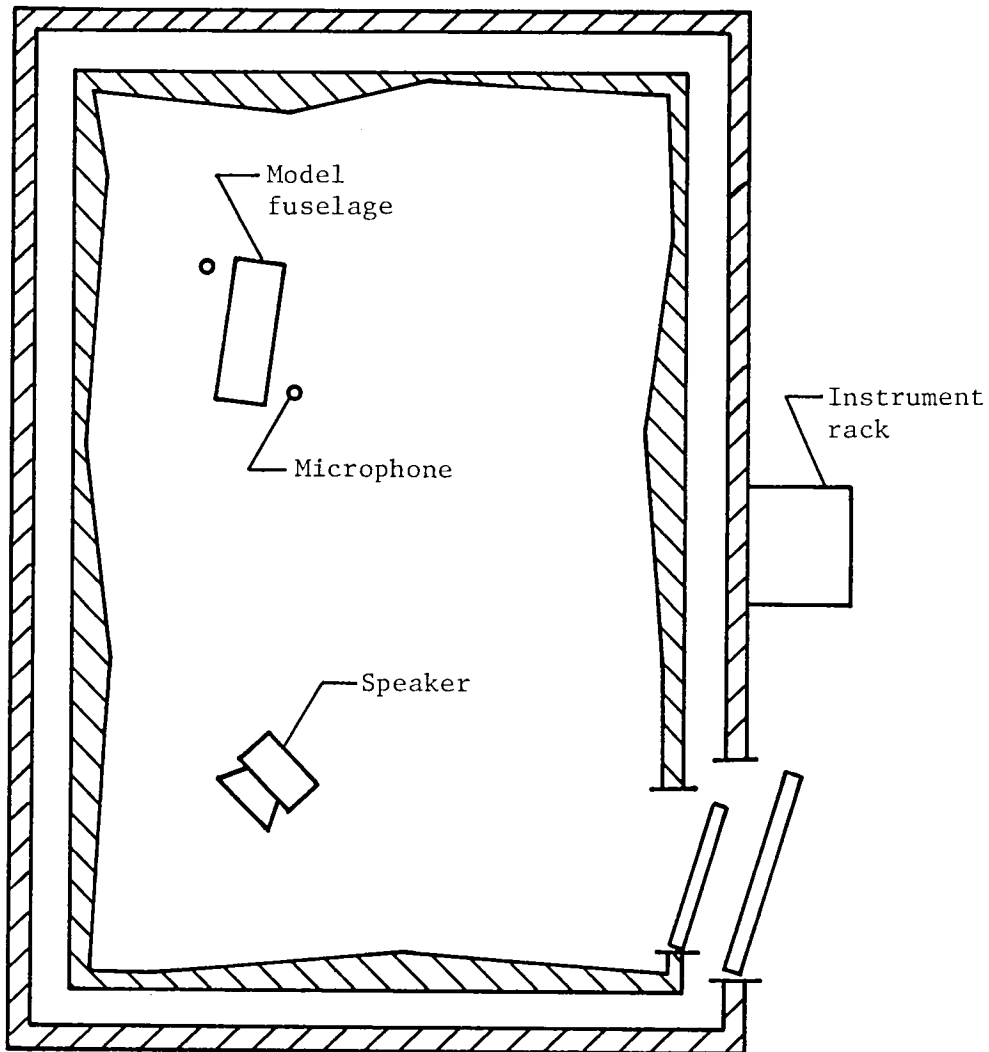
1. An unstiffened fuselage with no lining provided more noise reduction than a stiffened fuselage of the same size and weight.
2. The application of a lining to the fuselage tends to smooth out the interior-noise spectrum and reduce or mask some of the noise associated with resonant structural response.
3. A prediction program being developed concurrently (by Pope) with the present experimental investigation provides good estimates of noise reduction and can be used over a wider frequency range than simpler methods such as mass-law calculations.

Langley Research Center  
National Aeronautics and Space Administration  
Hampton, VA 23665  
January 26, 1984

## REFERENCES

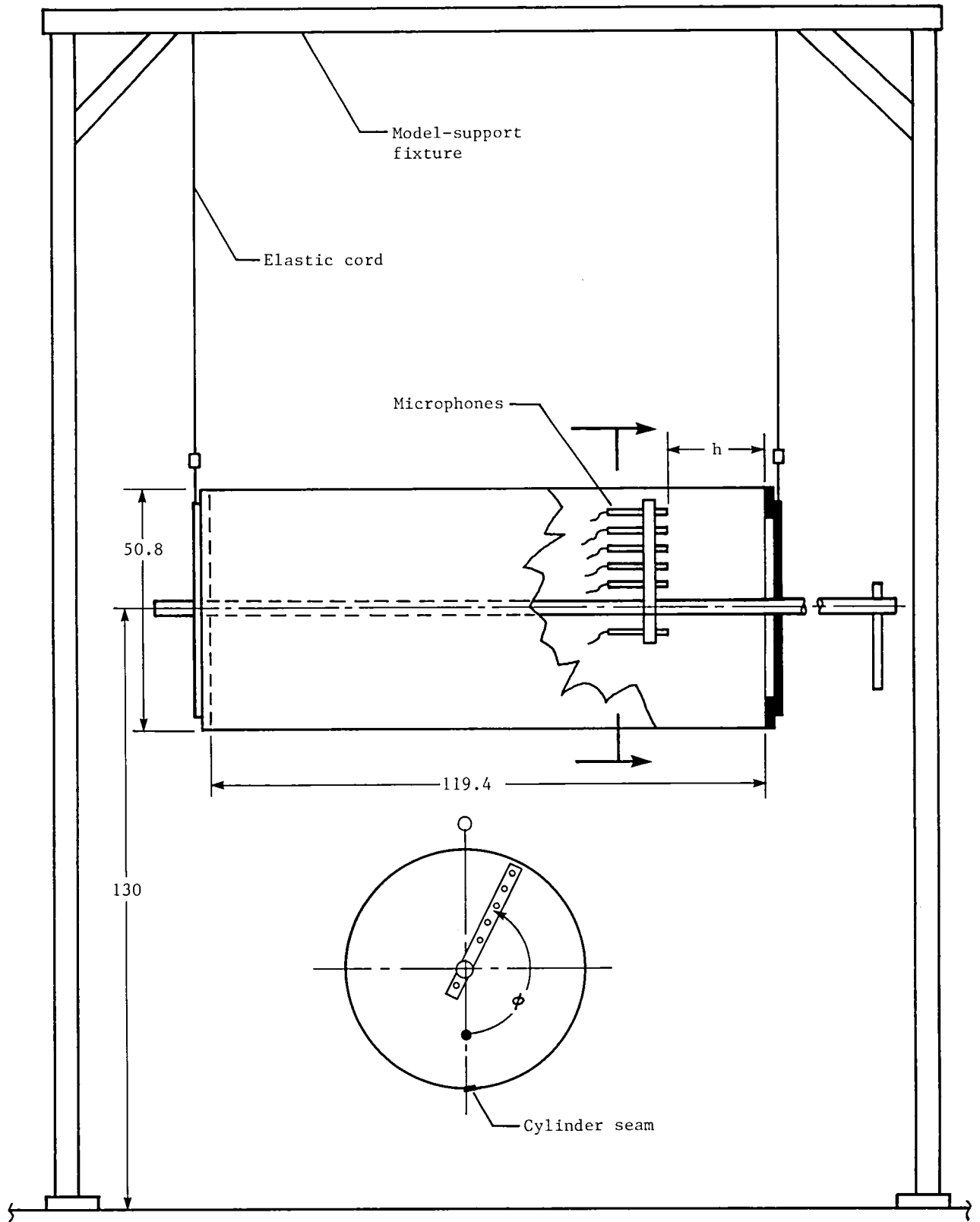
1. Wilby, John F.: Interior Noise of General Aviation Aircraft. SAE Tech. Paper Series 820961, Aug. 1982.
2. Metzger, Frederick B.: Strategies for Aircraft Interior Noise Reduction in Existing and Future Propeller Aircraft. SAE Tech. Paper Series 810560, Apr. 1981.
3. Pope, L. D.; Rennison, D. C.; Willis, C. M.; and Mayes, W. H.: Development and Validation of Preliminary Analytical Models for Aircraft Interior Noise Prediction. J. Sound & Vib., vol. 82, no. 4, June 22, 1982, pp. 541-575.
4. Willis, Conrad M.; and Daniels, Edward F.: Experimental Study of Noise Reduction for an Unstiffened Cylindrical Model of an Airplane Fuselage. NASA TP-1964, 1981.
5. Pope, L. D.; and Wilby, E. G.: Analytical Prediction of the Interior Noise for Cylindrical Models of Aircraft Fuselages for Prescribed Exterior Noise Fields. Phase II: Models for Sidewall Trim, Stiffened Structures, and Cabin Acoustics With Floor Partition. NASA CR-165869, 1982.
6. Hubbard, Harvey H.; and Manning, James C.: Aeroacoustic Research Facilities at NASA Langley Research Center - Description and Operational Characteristics. NASA TM-84585, 1983.
7. Mueller, Arnold W.: A Description and Some Measured Acoustic Characteristics of the Langley 220 Cubic Meter Reverberation Chamber. NASA TM X-72775, 1975.
8. McGary, Michael C.: Sound Field Diffusivity in NASA Langley Research Center Hardwalled Acoustic Facilities. NASA TM-83275, 1982.
9. Mixson, J. S.; Roussos, L. A.; Barton, C. K.; Vaicaitis, R.; and Slazak, M.: Laboratory Study of Efficient Add-On Treatments for Interior Noise Control in Light Aircraft. AIAA Paper 81-1969, Oct. 1981.
10. Pope, L. D.; Wilby, E. G.; Willis, C. M.; and Mayes, W. H.: Aircraft Interior Noise Models: Sidewall Trim, Stiffened Structures, and Cabin Acoustics With Floor Partition. J. Sound & Vib., vol. 89, no. 3, Aug. 8, 1983, pp. 371-417.

Splayed walls,  $6 \times 9 \times 4$  m;  
range, 50 to 20 000 Hz;  
reverberation time, 8 sec



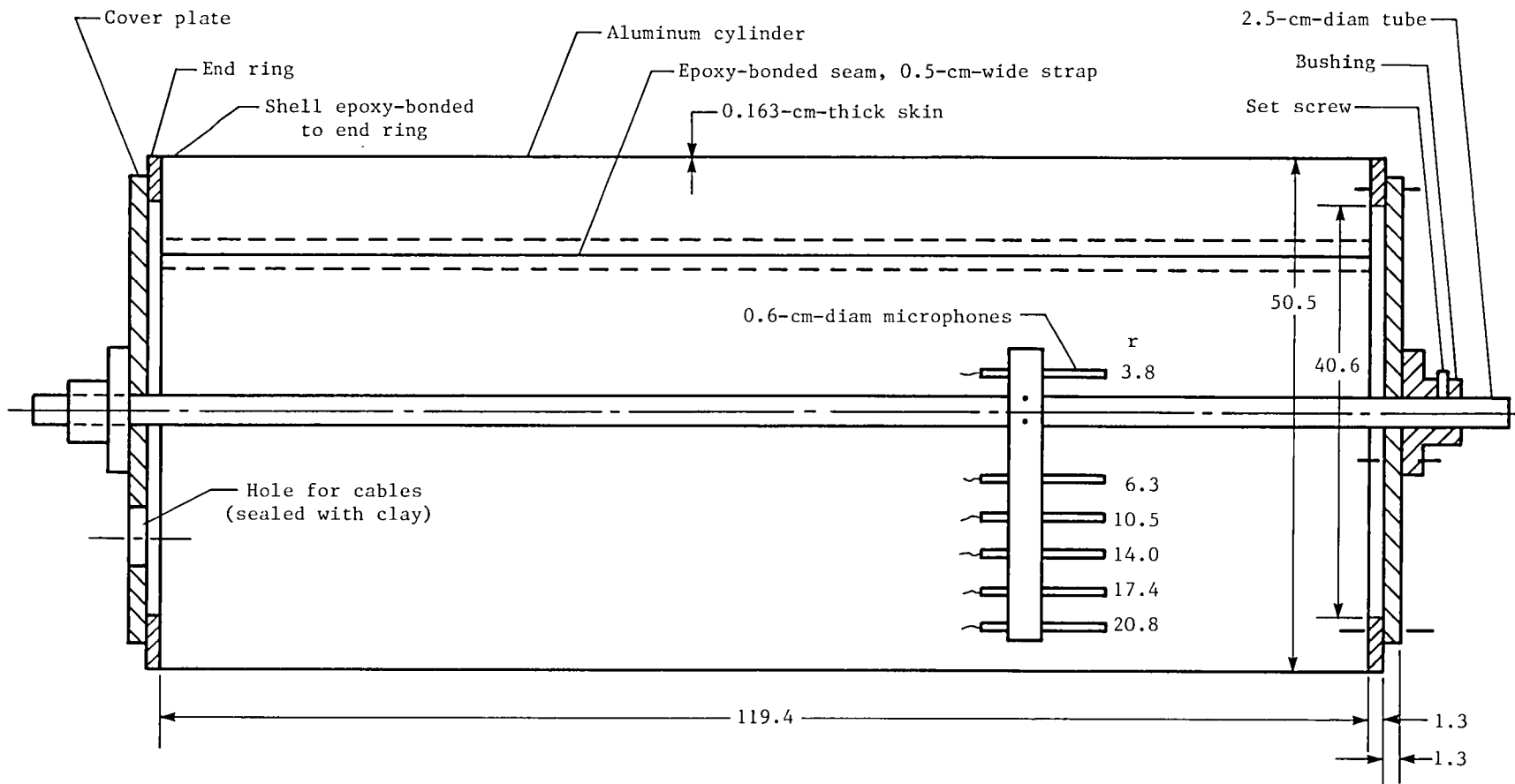
(a) Plan view of reverberation room.

Figure 1.- Schematic diagrams of test facilities and apparatus.



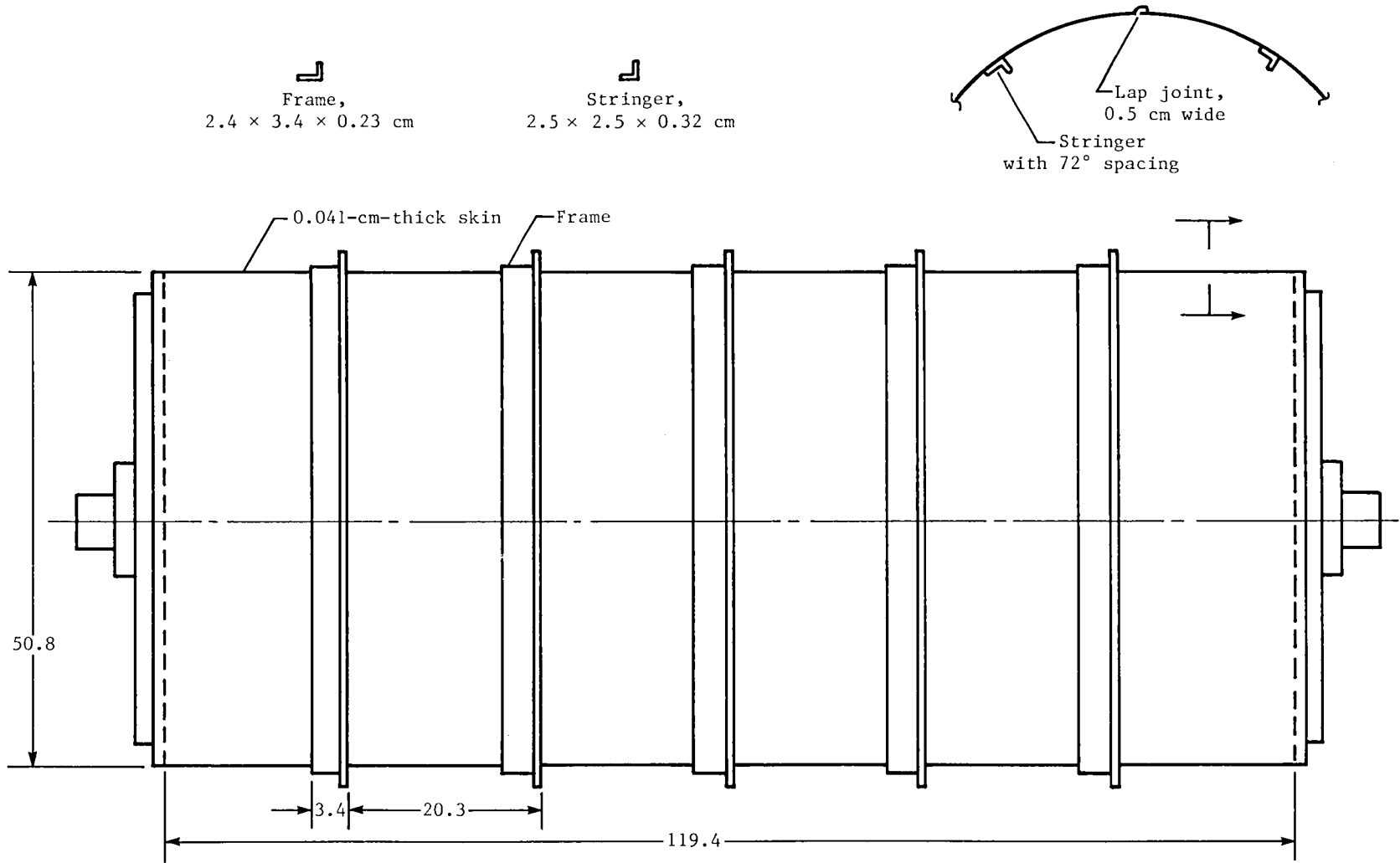
(b) Arrangement of apparatus. Dimensions are given in centimeters.

Figure 1.- Concluded.



(a) Unstiffened fuselage with floor removed.

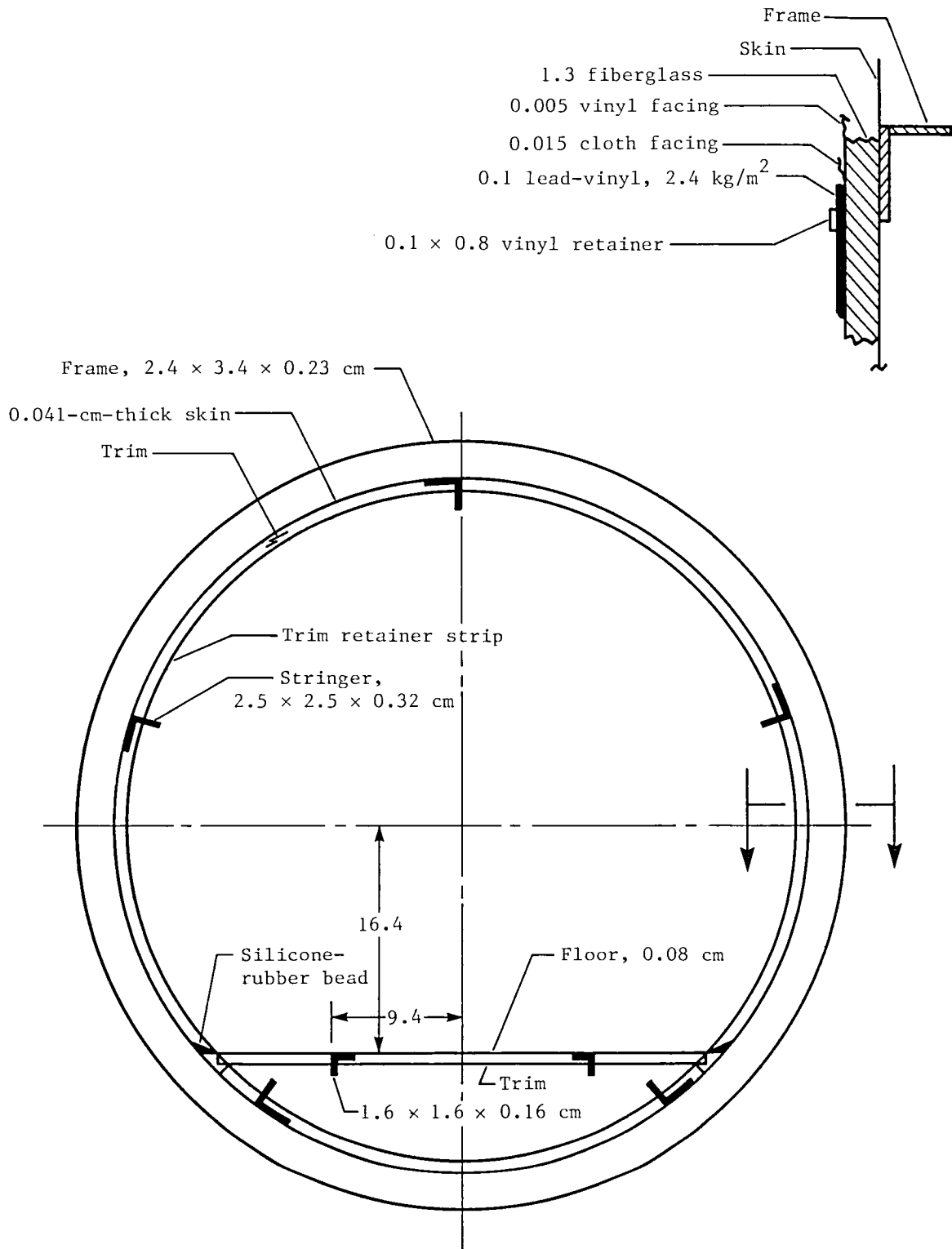
Figure 2.- Model details and microphone locations. Dimensions are given in centimeters.



(b) Stiffened fuselage.

Figure 2.- Continued.





(c) Cross section of stiffened fuselage with floor and lining installed.

Figure 2.- Concluded.

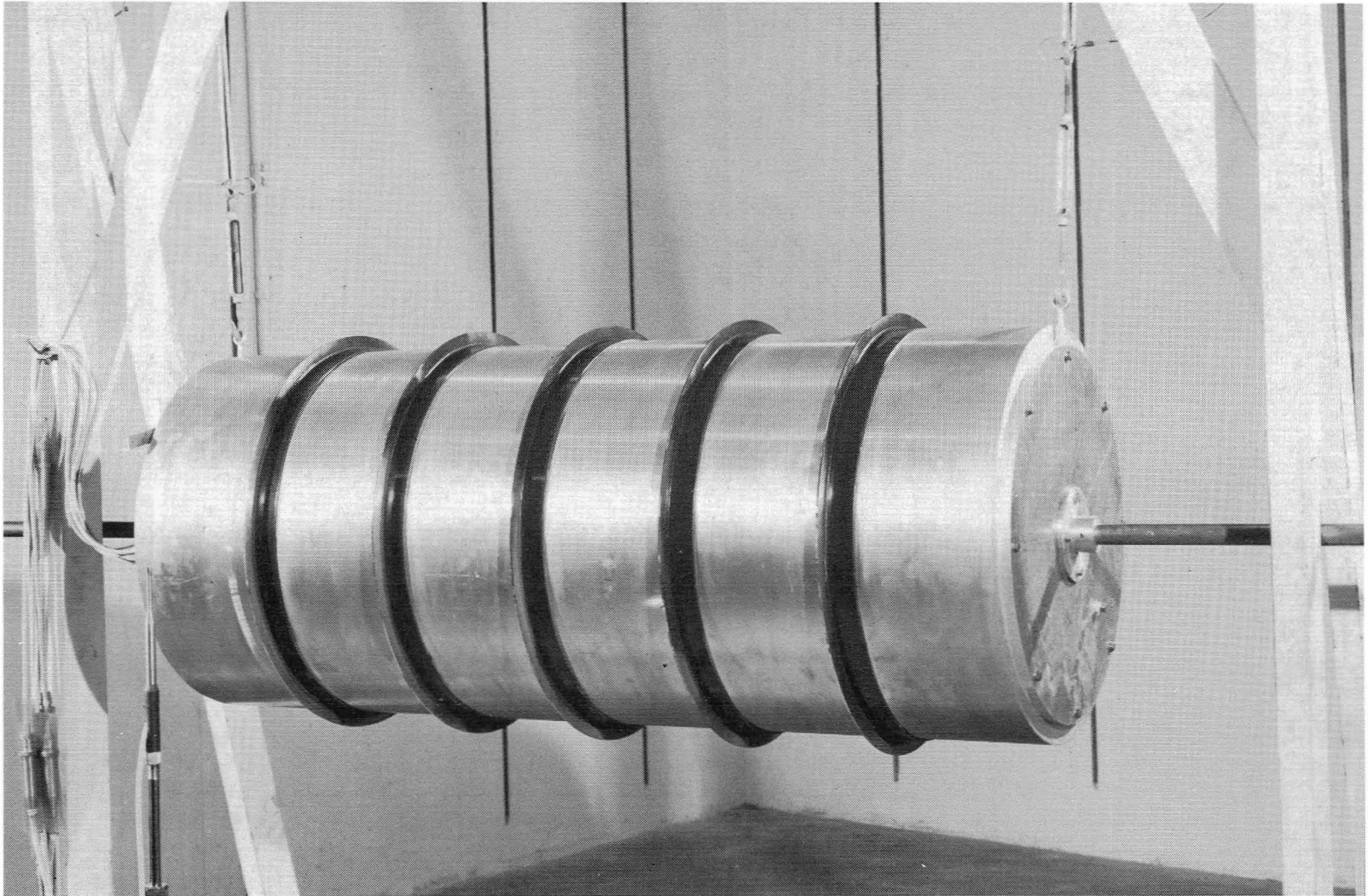


Figure 3.- Photograph of stiffened fuselage.

L-81-2440

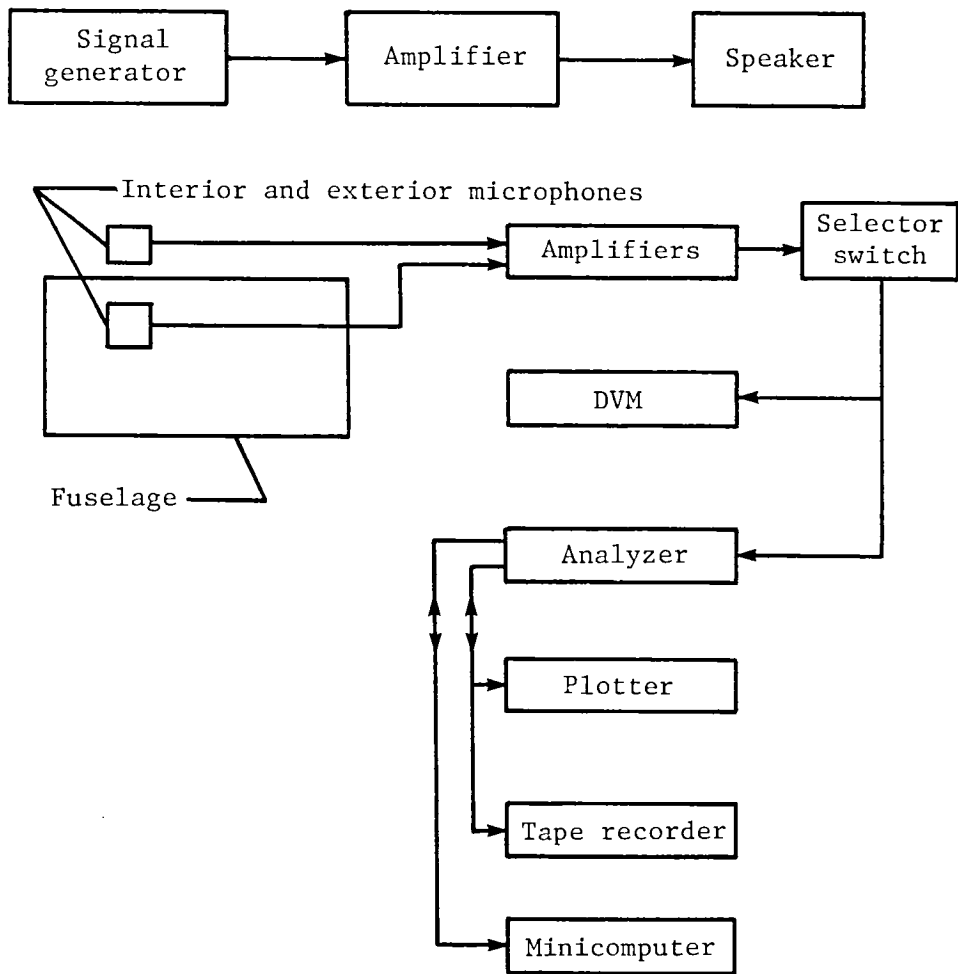


Figure 4.- Schematic diagram of instrumentation.

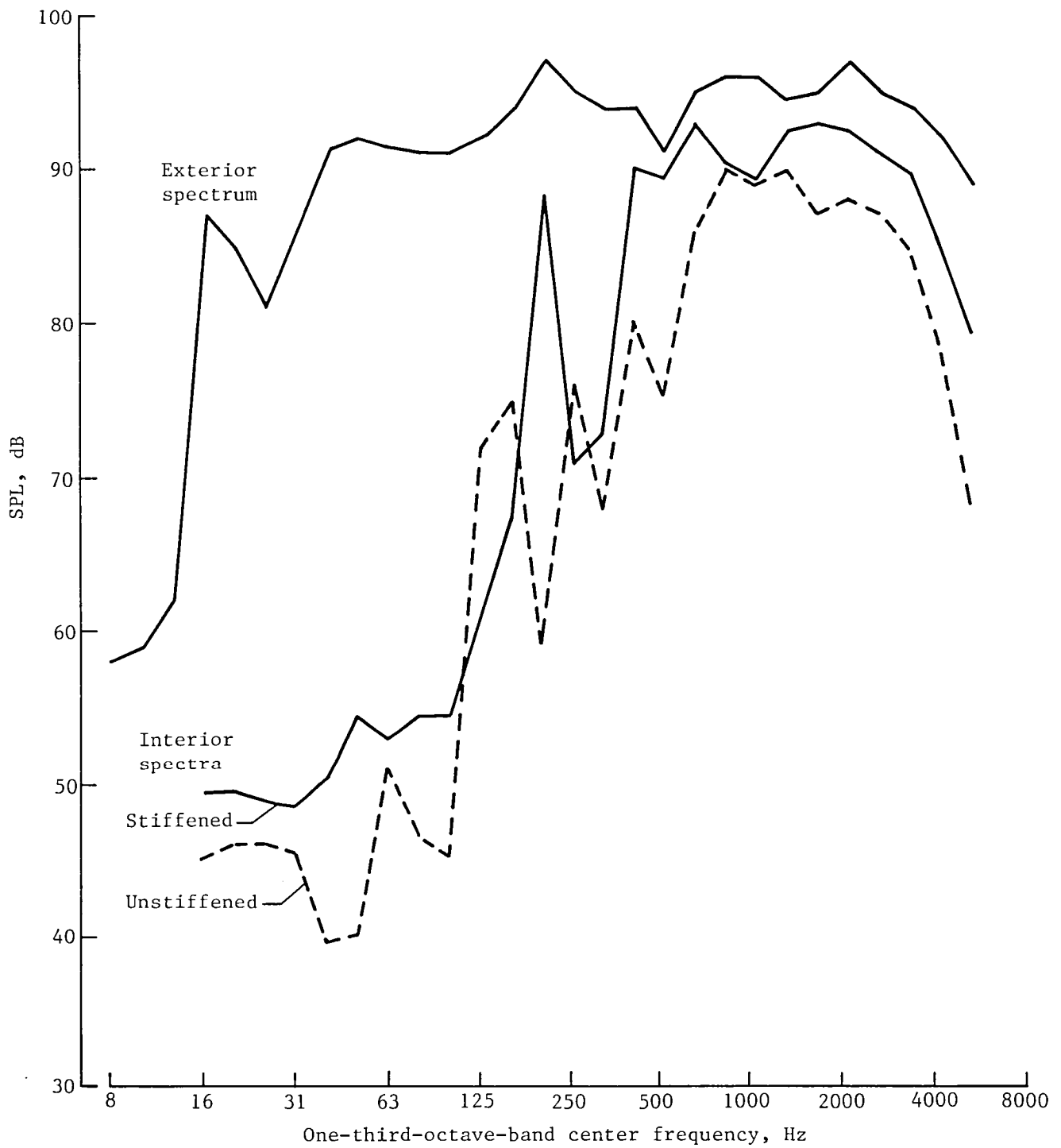


Figure 5.- Typical exterior and interior spectra for stiffened and unstiffened fuselages.  $r/R = 0.82$ .

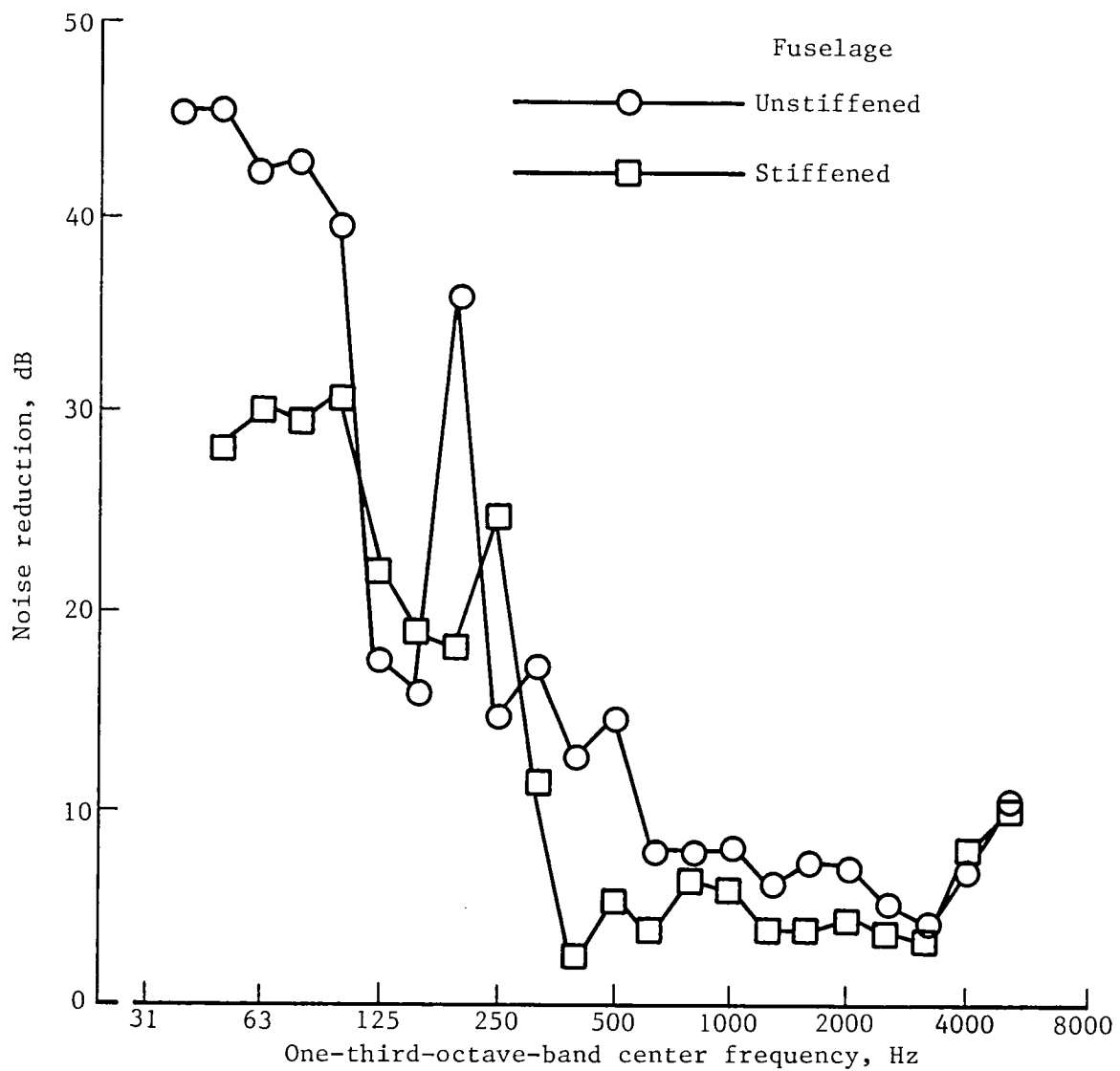
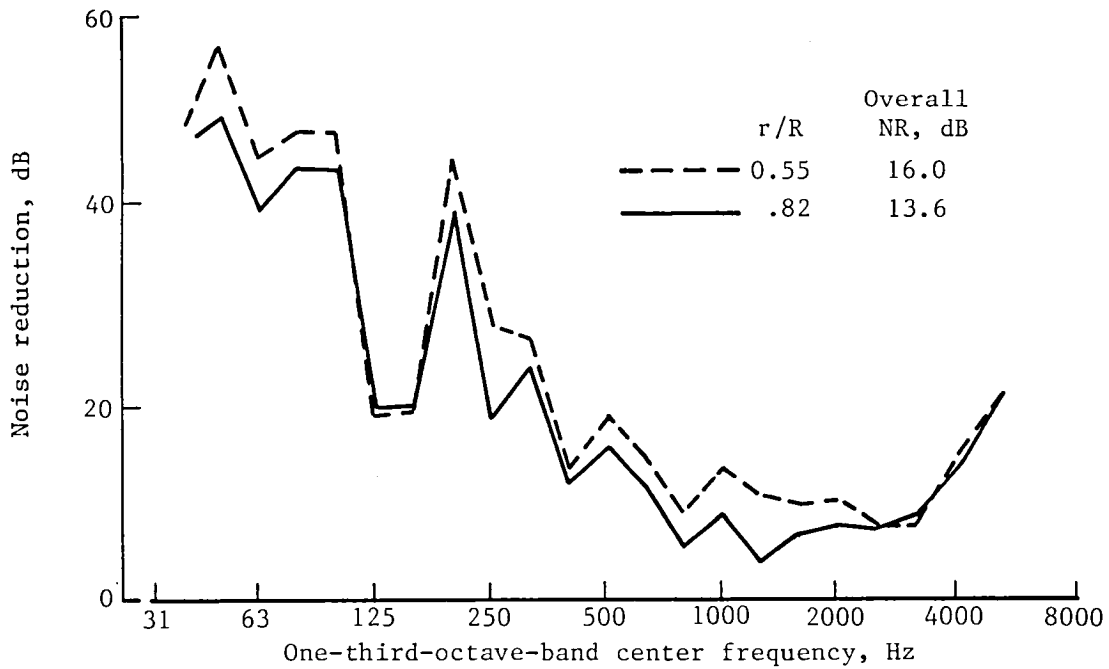
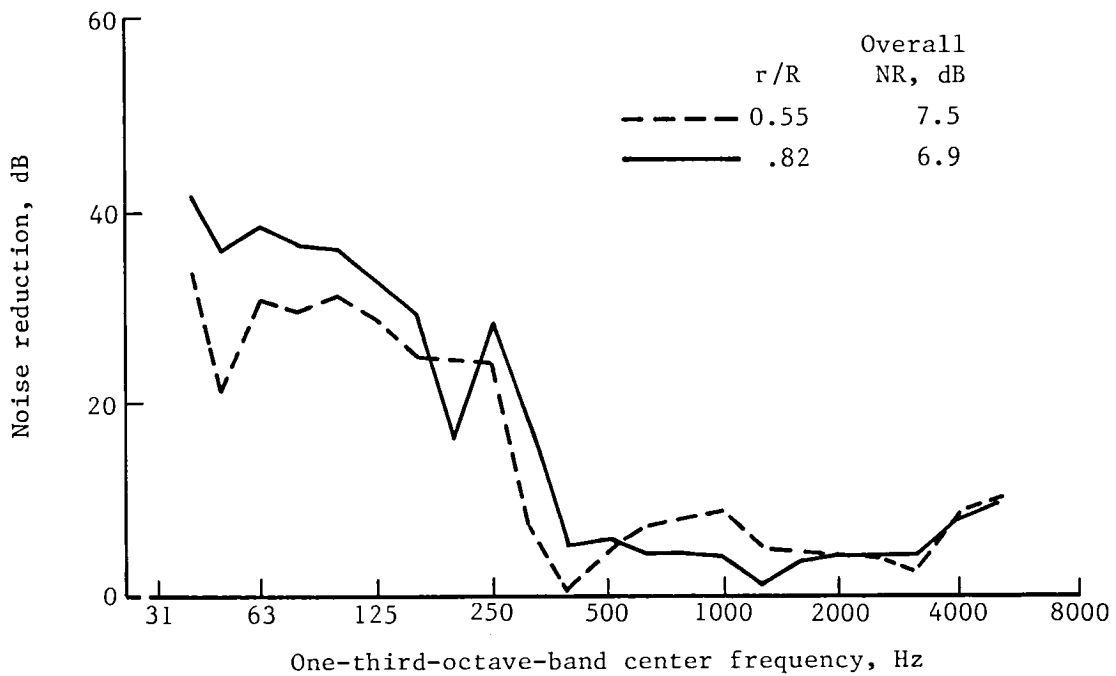


Figure 6.- Measured space-averaged noise reduction. Data taken from references 3 and 5.

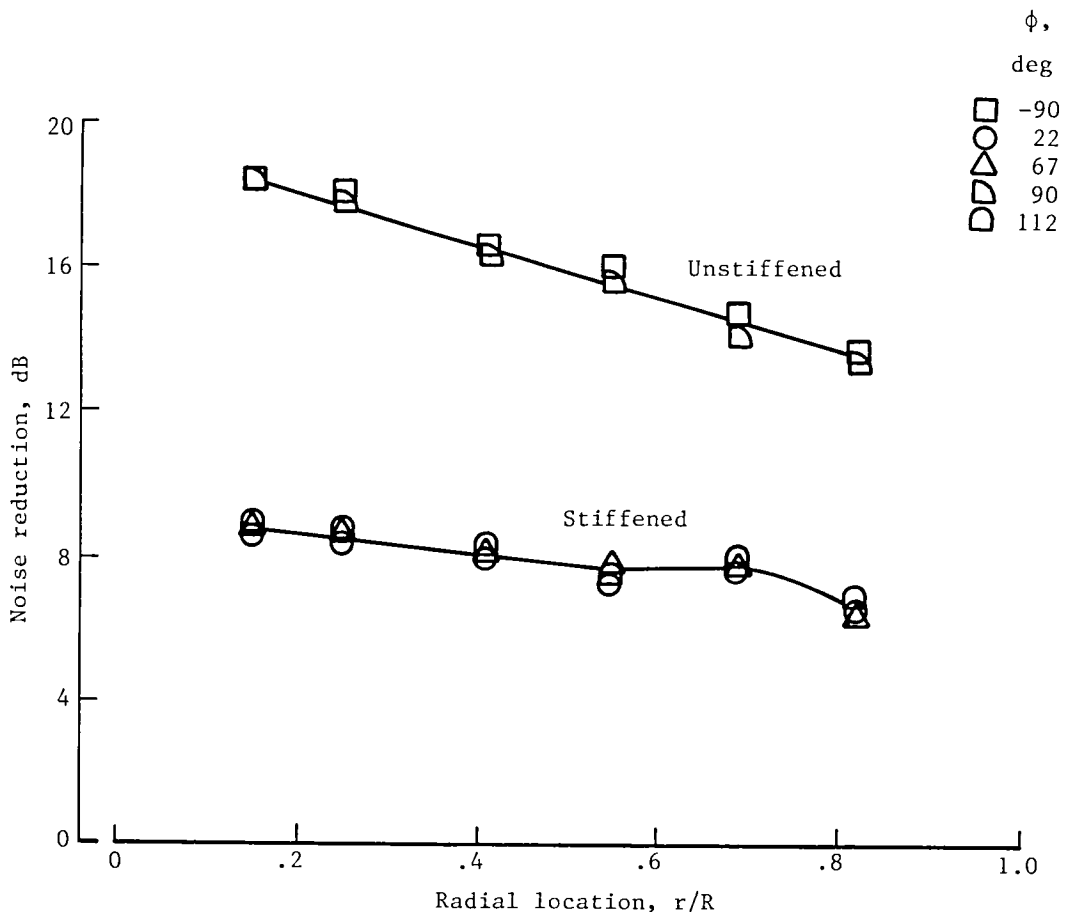


(a) Unstiffened fuselage.

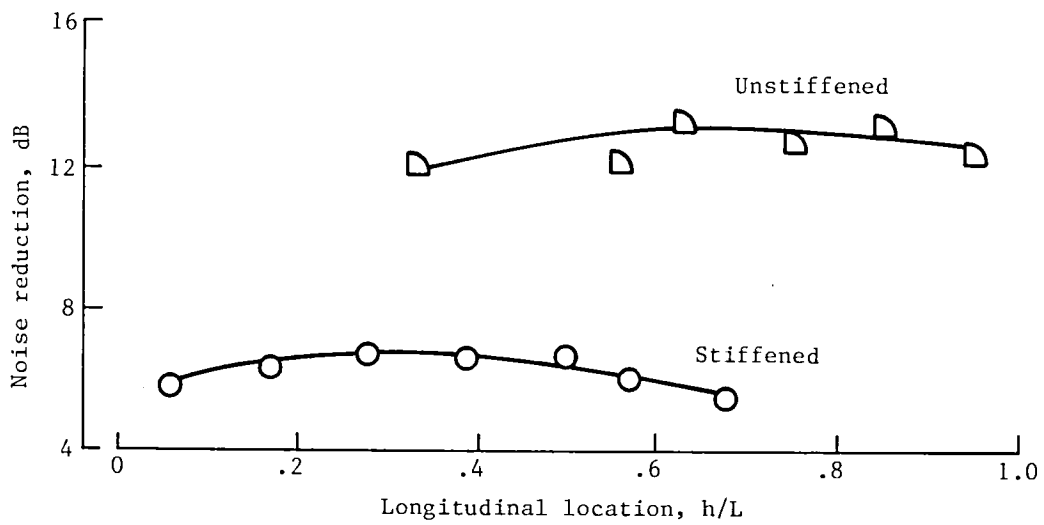


(b) Stiffened fuselage.

Figure 7.- Noise reduction at two radial locations.

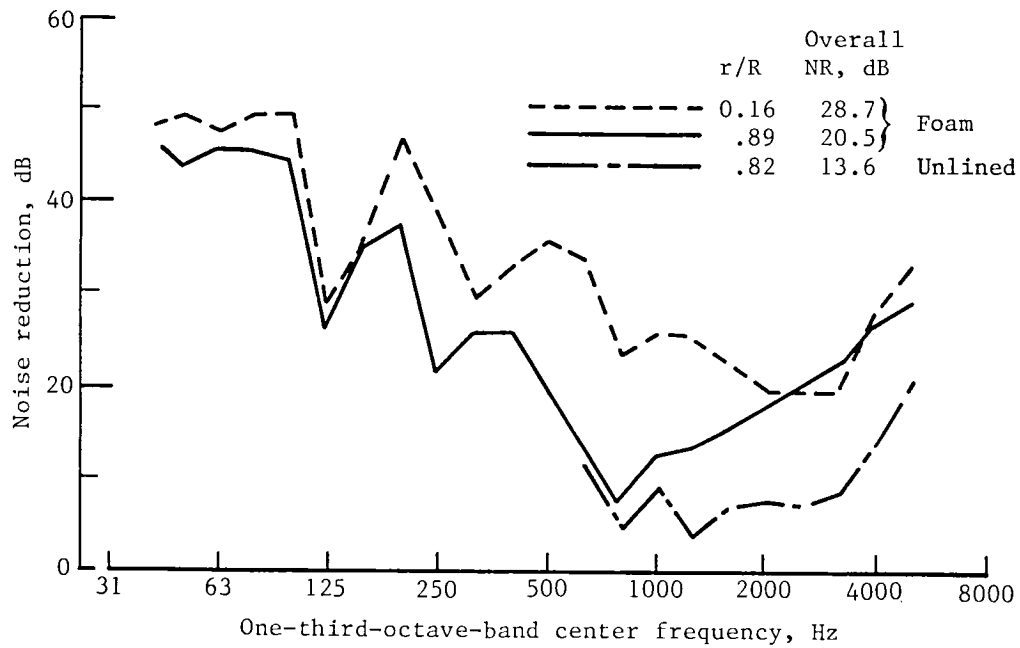


(a) Effect of radial location.  $h/L = 0.4$ .

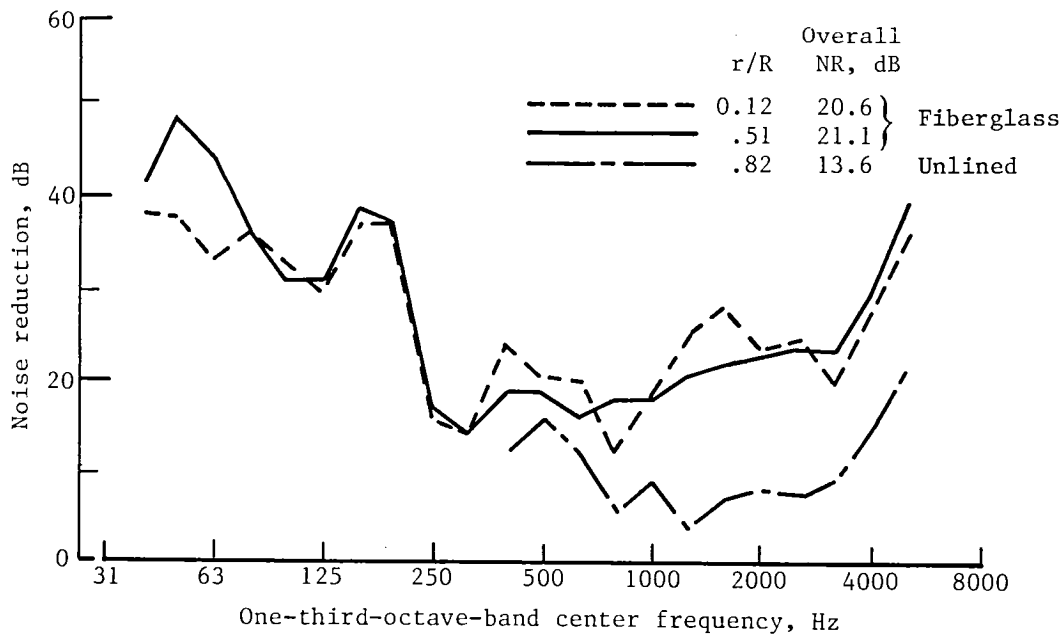


(b) Effect of longitudinal location.  $r/R = 0.82$ .

Figure 8.- Comparison of noise reduction for stiffened and unstiffened fuselages.



(a) Fuselage lined with 0.6-cm-thick acoustic foam.



(b) Fuselage with floor and with 1.3-cm-thick fiberglass.

Figure 9.- Noise-reduction spectra for unstiffened fuselage with and without lining.



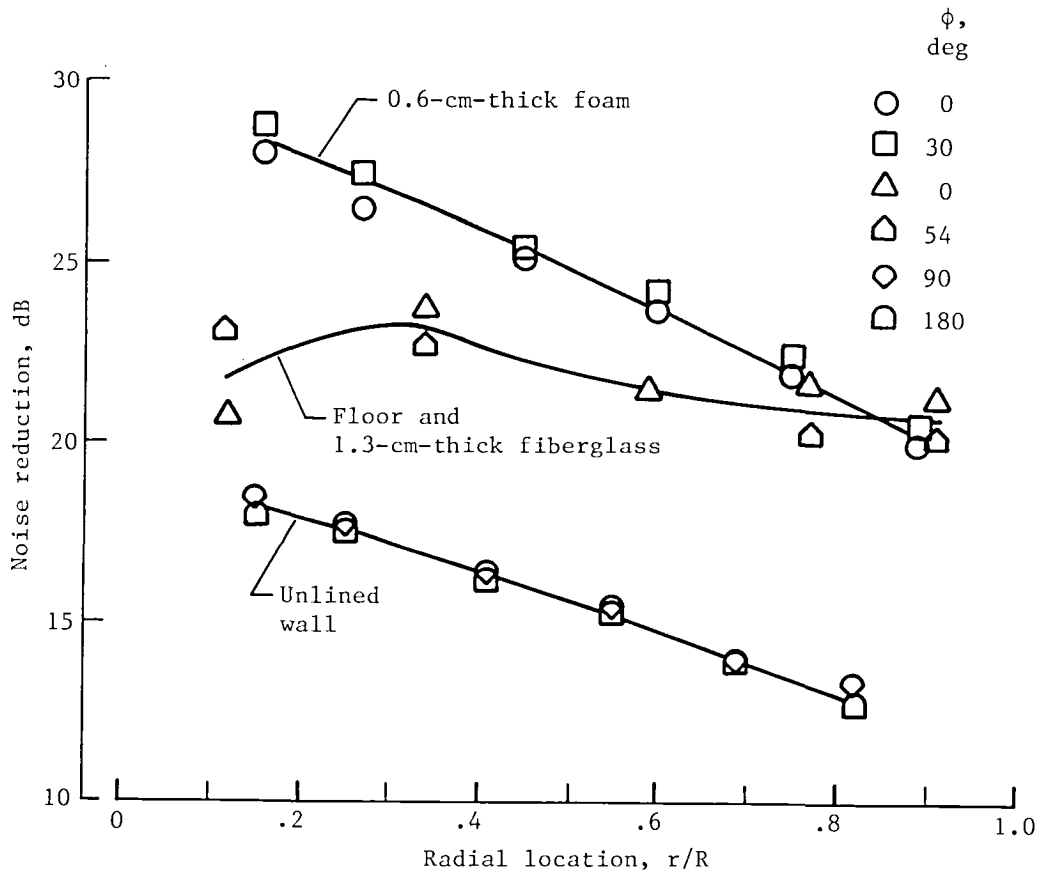


Figure 10.- Radial variation of noise reduction for unstiffened fuselage with and without lining.

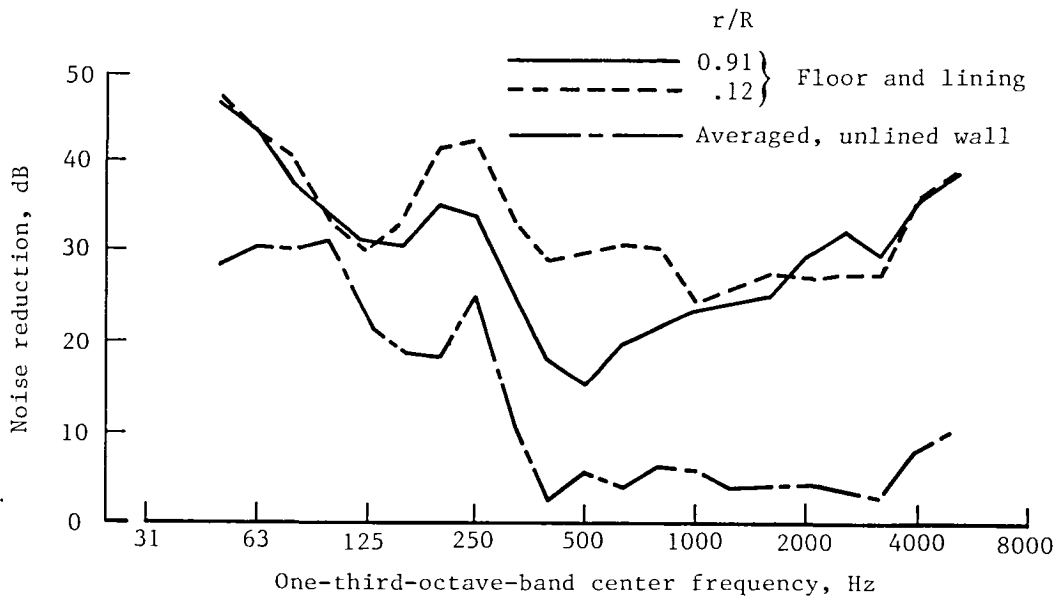
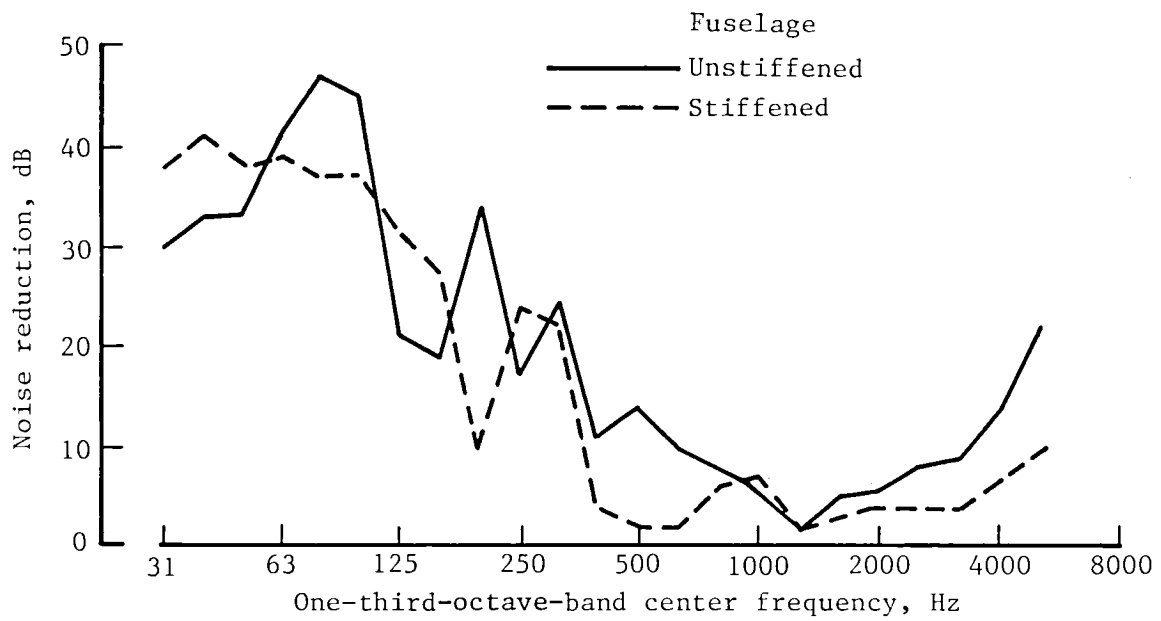
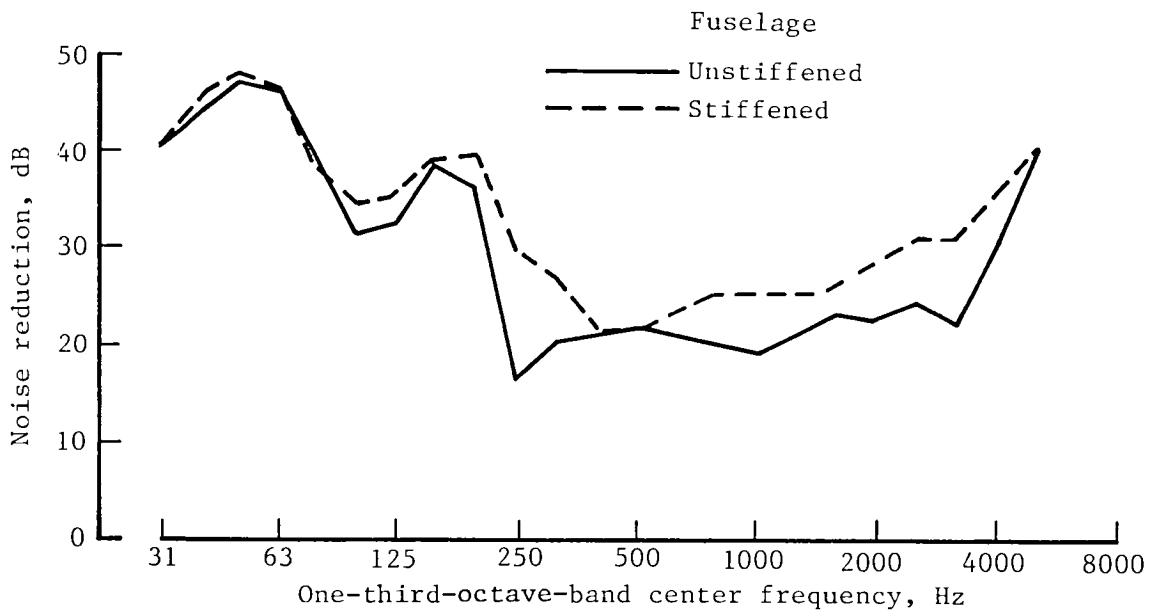


Figure 11.- Noise-reduction spectra for stiffened fuselage with floor and lining.



(a) Unlined fuselage.



(b) Lined fuselage with floor installed.

Figure 12.- Comparison of noise reduction for stiffened and unstiffened fuselages.

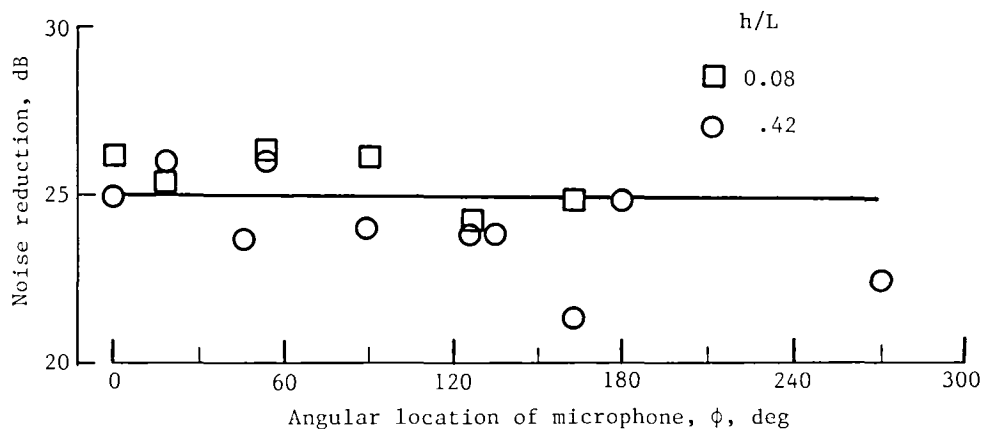


Figure 13.- Circumferential variation in noise reduction for stiffened fuselage with floor and lining.

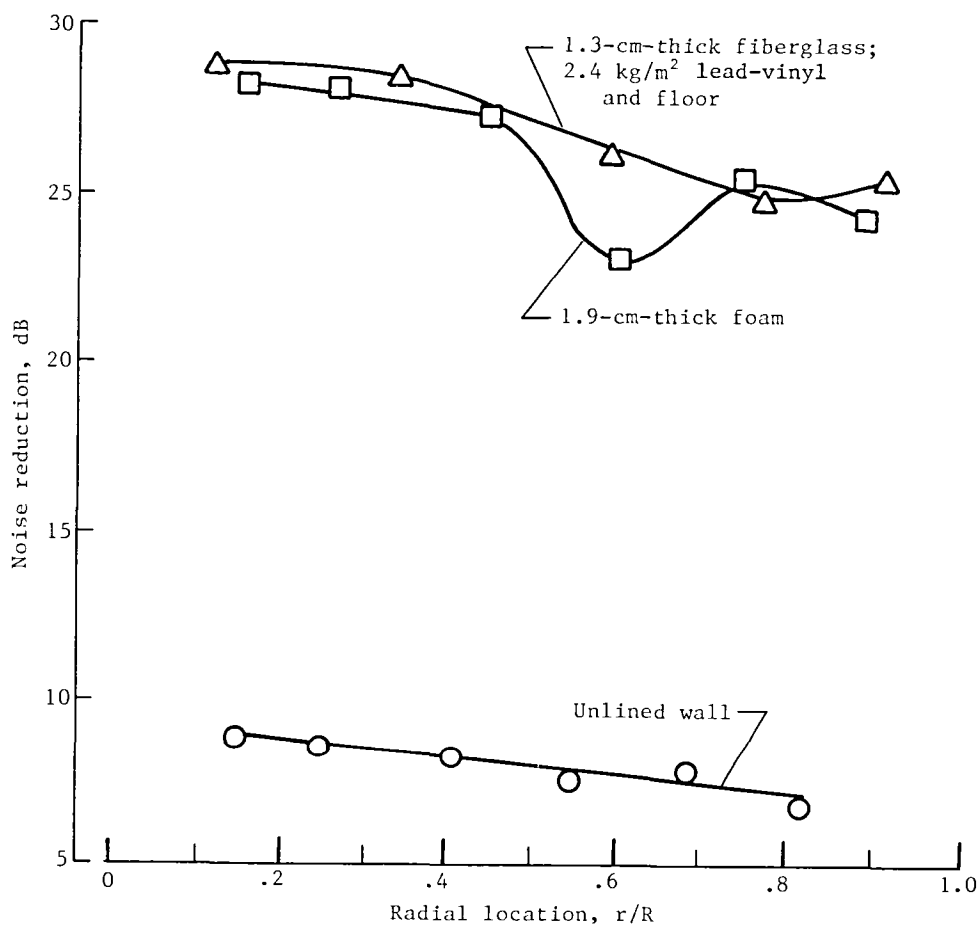
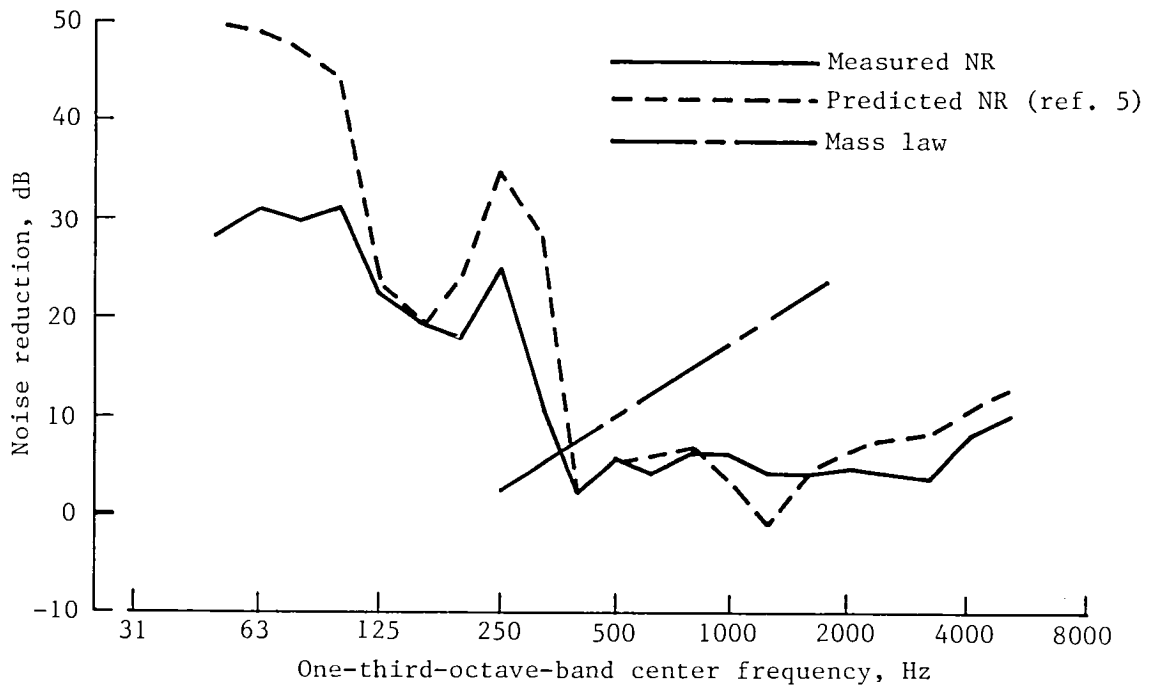
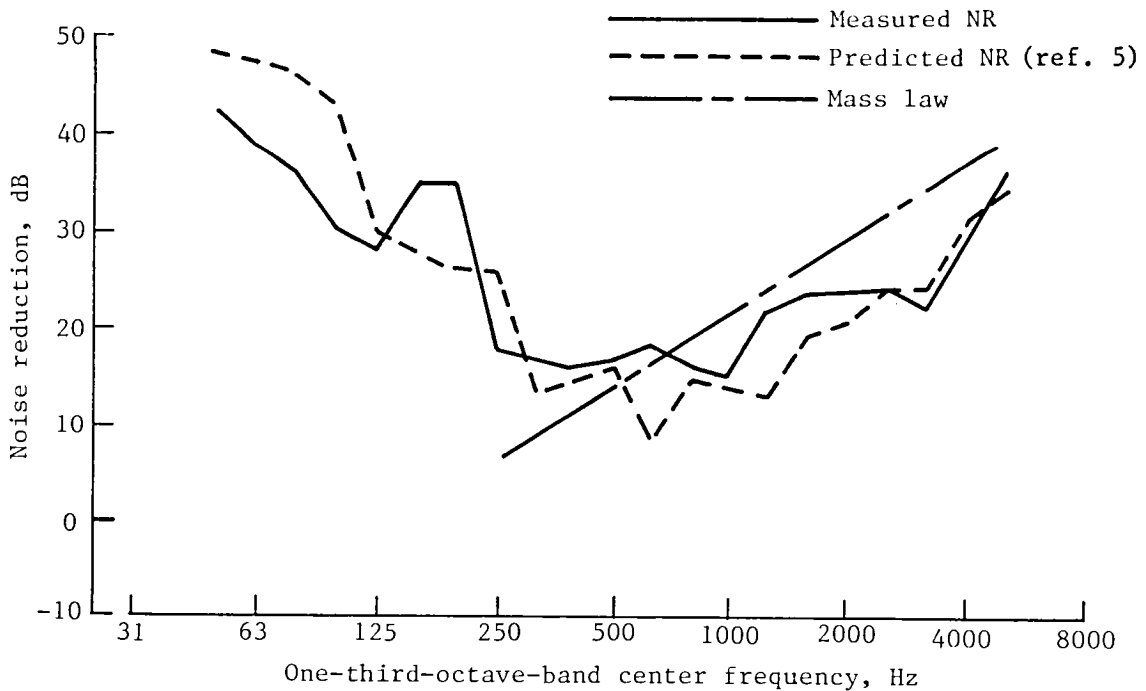


Figure 14.- Radial variation of noise reduction for stiffened fuselage with and without lining.

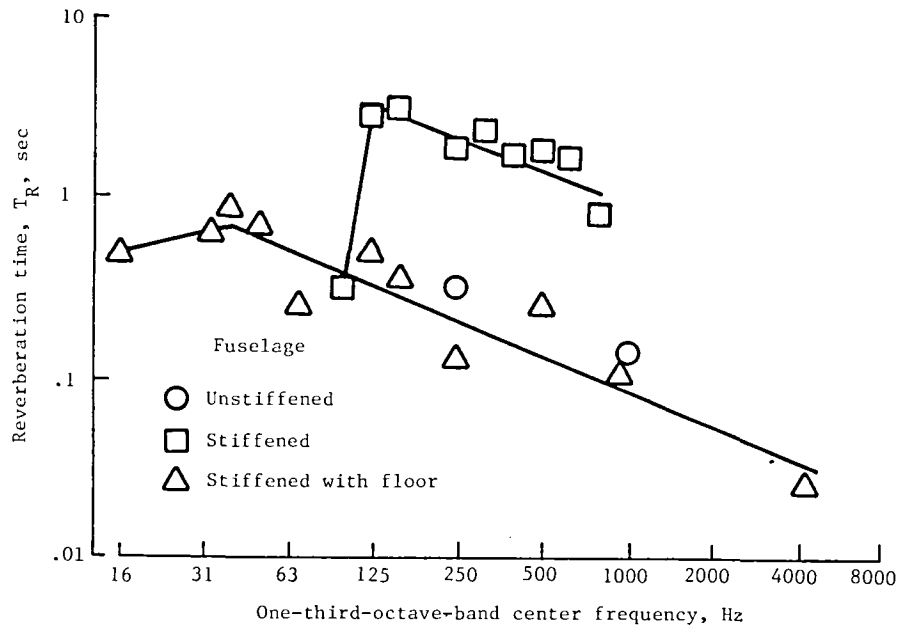


(a) Unlined stiffened fuselage.

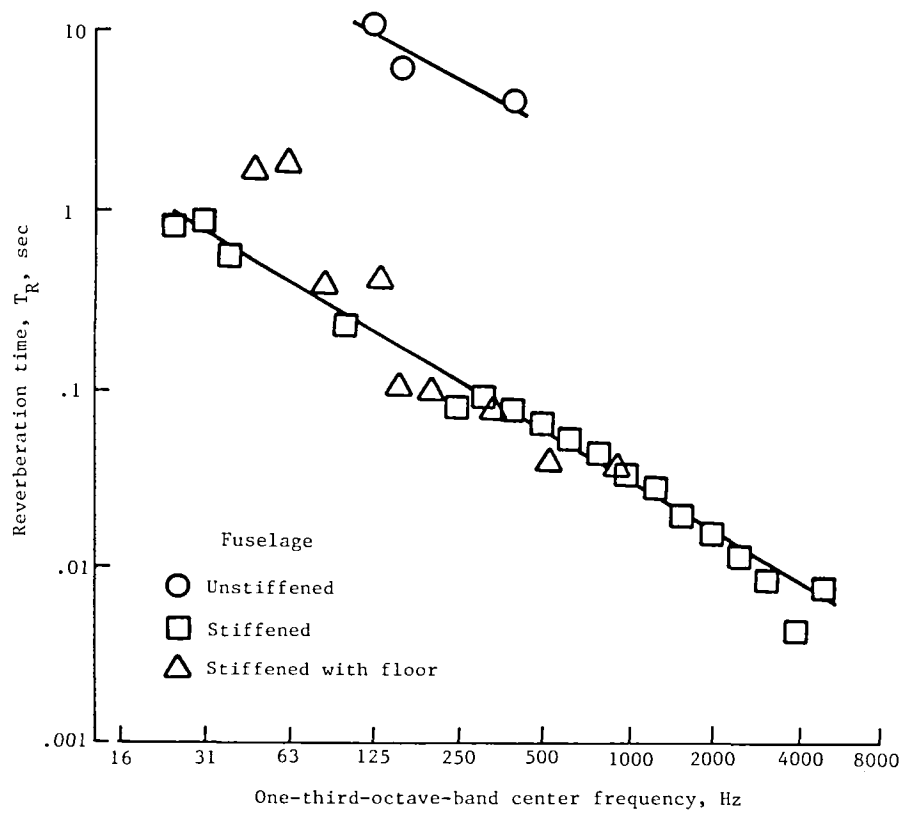


(b) Lined unstiffened fuselage with 1.3-cm-thick fiberglass.

Figure 15.- Comparison of measured space-averaged noise reduction with predictions for lined and unlined fuselages.



(a) Acoustic reverberation time.



(b) Structural reverberation time.

Figure 16.- Comparison of reverberation times for stiffened and unstiffened fuselages.

1. Report No. NASA TM-85716		2. Government Accession No.		3. Recipient's Catalog No.	
4. Title and Subtitle NOISE-REDUCTION MEASUREMENTS ON STIFFENED AND UNSTIFFENED CYLINDRICAL MODELS OF AN AIRPLANE FUSELAGE				5. Report Date February 1984	
				6. Performing Organization Code 505-33-53-03	
7. Author(s) Conrad M. Willis and William H. Mayes				8. Performing Organization Report No. L-15699	
9. Performing Organization Name and Address NASA Langley Research Center Hampton, VA 23665				10. Work Unit No.	
				11. Contract or Grant No.	
12. Sponsoring Agency Name and Address National Aeronautics and Space Administration Washington, DC 20546				13. Type of Report and Period Covered Technical Memorandum	
				14. Sponsoring Agency Code	
15. Supplementary Notes					
16. Abstract  Noise-reduction measurements are presented for a stiffened and an unstiffened model of an airplane fuselage. The cylindrical models were tested in a reverberant-field noise environment over a frequency range from 20 Hz to 6 kHz. An unstiffened metal fuselage provided more noise reduction than a fuselage having the same sidewall weight divided between skin and stiffening stringers and ring frames. The addition of acoustic insulation to the models tended to smooth out the interior-noise spectrum by reducing or masking the noise associated with the structural response at some of the resonant frequencies.					
17. Key Words (Suggested by Author(s)) Interior noise Noise reduction			18. Distribution Statement Unclassified - Unlimited  Subject Category 71		
19. Security Classif. (of this report) Unclassified		20. Security Classif. (of this page) Unclassified		21. No. of Pages 26	22. Price A03



National Aeronautics and  
Space Administration

Washington, D.C.  
20546

Official Business

Penalty for Private Use, \$300

THIRD-CLASS BULK RATE

Postage and Fees Paid  
National Aeronautics and  
Space Administration  
NASA-451



**NASA**

POSTMASTER: If Undeliverable (Section 158  
Postal Manual) Do Not Return

---